RESEARCH

Distribution feature and development characteristics of geohazards in Wudu district, Gansu province, Northwest China

Shuai Zhang[1,2,3], Ping Sun[1,2,3*], Ran Li[1,2,3], Yanlin Zhang[4] and Jian Ren[1,2,3]

Abstract

Background: The study area located at southeast Gansu, China, has long been afflicted by the intense occurrence of geohazards. The study area is characterized by interleaving terrain of precipitous mountains and valley basins, abundant precipitation, and complicated geological setting. In this work, 1144 geohazards including 759 landslides, 281 debris flows, and 104 collapse were presented and their types were categorized in detail. Then, the distribution of geohazards were analyzed and the controlling role of hazard-inducing environment and triggering factors on geohazards were preliminary presented.

Results: In this work, correlation analysis between geohazards and geological, topographical, and geomorphological context was conducted. Concave slopes with height smaller than 200 m and slope gradient between 21° and 40° is the favorable topographic feature for landslide occurrence and the predominant slope aspects of landslides are southwest, south, west, and southeast. Collapse generally occurs in slope with gradient larger than 45°. Valleys with valley gradient less than 400‰, valley height between 100 and 500 m, and watershed area of 1–10 km^2 register the largest percentage and the most favorable slope gradient for the supply of solid source at the debris flow source area is 25°–45°. The preferable strata for geohazards (landslide, collapse and debris flow) are Middle and upper Pleistocene loess, Holocene diluvium, Silurian phyllite and slate, Neogene mudstone, and Devonian schist and gneiss, and most geohazards occurred in tectonic erosional middle altitude mountain, tectonic erosional high-middle altitude mountain, tectonic erosional-diluvial planation surface. In addition, the controlling role of triggering factors, i.e., precipitation, earthquake, and human engineering activity was discussed and described in this work.

Conclusion: Geohazards in the study area are synthetically controlled by the hazard-inducing environment and triggering factors. The complicated sliding-prone strata and steep topography resulted from strong tectonic movement provides a favorable basis for the development and formation of geohazards. Heavy rainfall, strong seismic motion, and human engineering activity are the main triggering factors for geohazard occurrence.

Keywords: Geohazard, Wudu district, Geohazard type, Spatial distribution, Controlling factor

Introduction

Geohazards triggered by extreme precipitation and strong earthquake are a main threat to the society and properties due to the abrupt and massive occurrence in the world. Research on the spatial distribution, hazard-inducing environment, and triggering factors of massive geohazards is the basis of failure mechanism and runout prediction, and can provide useful insight into mitigation and reduction of geohazards. In previous work, most

*Correspondence: sunpingcgs@foxmail.com

[1] Institute of Geomechanics, Chinese Academy of Geological Sciences, Beijing 100081, China
Full list of author information is available at the end of the article
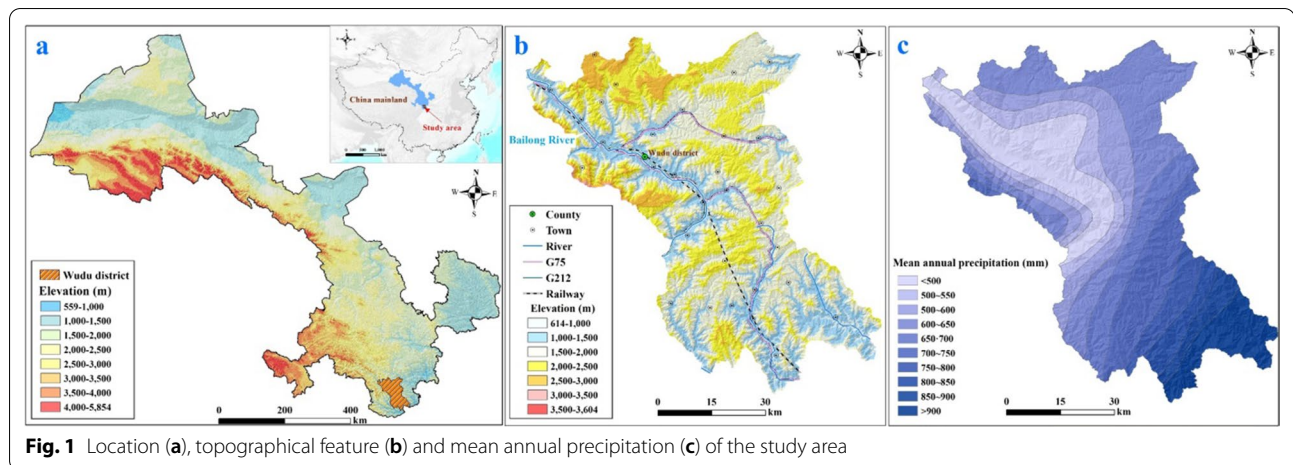
Fig. 1 Location (**a**), topographical feature (**b**) and mean annual precipitation (**c**) of the study area

studies focused on massive geohazards triggered by a certain event (such as the 2008 Wenchuan Earthquake, the 2017 Jiuzhaigou earthquake, the 2018 Hokkaido Eastern Iburi earthquake) (Qi et al. 2010; Gorum et al. 2011; Xu et al. 2015; Fan et al. 2018; Zhang et al. 2019). The analysis of spatial distribution of massive geohazards and their controlling factors in a certain event is of great importance since correlation between geohazards and triggering factors can be clearly evaluated. However, correlation analysis between triggering factors and massive geohazards those occurred in multiple stages generally show unsatisfied results as geohazards were triggered by different inducing factors and the contribution of different inducing factors varies in different events. In this situation, research on distribution feature and development characteristics of geohazards is important as it can help to definitely clarify the favorable hazard-inducing environment.

The study area is located at southeastern Gansu Province, China (Fig. 1a) and this area belongs to the transition zone from the second step to the third step of the Chinese continent. The strong tectonic motion shapes the high and steep topography in the study area which is favorable for geohazards and the frequently rainstorm exacerbates this situation. During the 2008 Wenchuan Earthquake, 516 geohazards were triggered in the study area based on the report provided by the local government. In August 2020, two successions of heavy precipitation triggered a large number of geohazards and resulted in a total economic loss of RMB 0.43 billion. In this context, numerous research concerning susceptibility analysis, rainfall threshold analysis, deformation response and geohazard detection were conducted in previous work (Bai et al. 2012; Bai et al. 2014; Zhang et al. 2016; Xie et al. 2017; Liu et al. 2022). The logistic regression model was applied in the study area to conduct the

susceptibility mapping on 505 rainfall-induced landslides from 1995 to 2003 and 555 landslides triggered by the 2008 Wenchuan Earthquake, respectively, and landslides distributed in different susceptibility zones were obtained (Bai et al. 2013). The antecedent soil water status (ASWS) model in combination with logistic regression was applied and the relation between maximum daily rainfall and the water storage within the soil from previous rainfall events was conducted (Bai et al. 2014). In terms of risk assessment in previous studies, risk assessment of geohazards at different scale was conducted in the study area. 3 representative quantitative methods (information value model, logistic regression model, and artificial neural network based on frequency ratio model) were used to evaluate the landslide hazard risk in the Bailong River Basin based on 272 historical landslides from the national landslide catalog and 10 influencing factors, (Liu and Wu 2020). In addition, risk assessment of debris flow under different rainfall condition were conducted considering runout distance and properties within the potential impact zone (Ouyang et al. 2019; Zhang et al. 2022). These studies provide useful insight for this work, but a relatively complete geohazard inventory is needed which can provide a general perspective for geohazard distribution and serve as a reference for mitigation and reduction in the study area. Considering the frequently occurred geohazards, it is necessary to investigate the distribution and hazard-inducing factors of geohazards based on a relatively complete geohazard inventory.

In this light, this work presents a geohazard inventory incorporating 1,144 geohazards (including 759 landslides, 281 debris flows, and 104 collapses) in Wudu district, Gansu province, Northwest China and correlation analysis between geohazards and hazard-inducing factors is investigated as well. Research on the distribution characteristics of the geohazards in the study area is expected
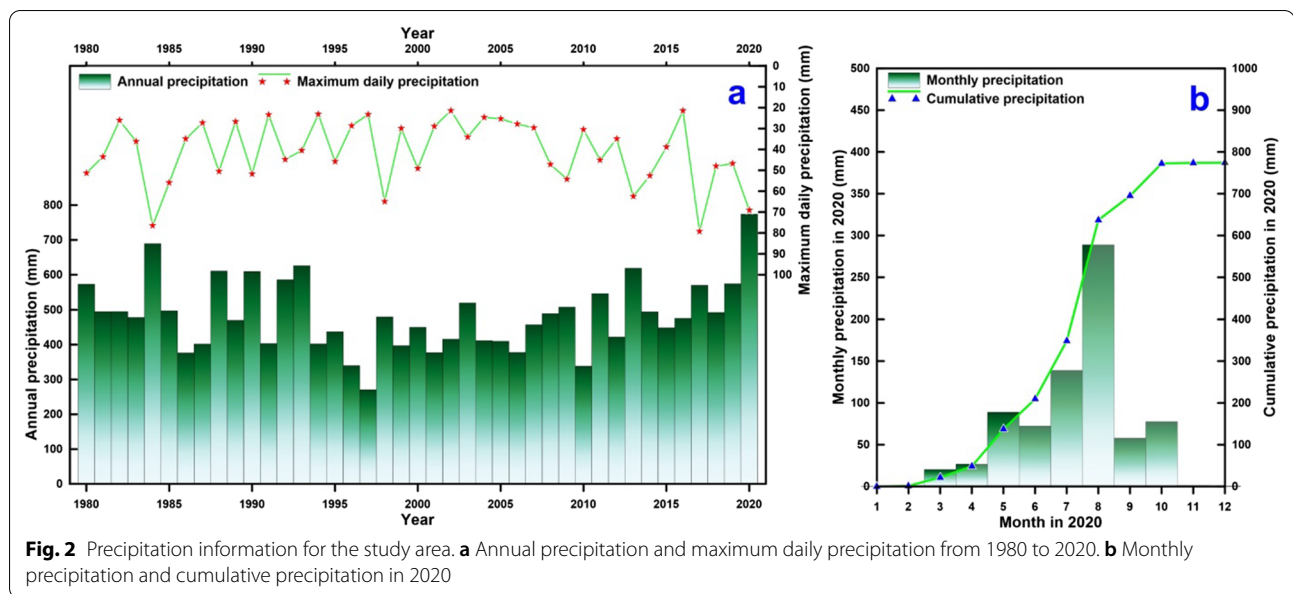
Fig. 2 Precipitation information for the study area. **a** Annual precipitation and maximum daily precipitation from 1980 to 2020. **b** Monthly precipitation and cumulative precipitation in 2020

to provide useful guidance for disaster relief operations, a macroscopic perspective for further mechanism research, and reference for hazard mitigation of similar scenarios in the future.

Research area
Climate and precipitation
The study area belongs to the middle reaches of the Bailong river, a first-class tributary of the Jialing River (Fig. 1a, b), and this area is situated at the transition zone from the humid subtropical monsoon to the warm subhumid climate (Ouyang et al. 2019). Due to the blockage of the South Qinling and Minshan Mountains, pronounced foehn effect can be observed in this area. Meanwhile, affected by steep topography, the climate varies vertically, and the precipitation increases with an increase in elevation (Zhang et al. 2022). Thus, the mean annual precipitation of study area is characterized by an escalating trend from northwest to southeast (Fig. 1c). In addition to the spatially uneven distribution of the annual precipitation, temporarily uneven distribution is another prominent feature. Based on the meteorological data (1980 to 2020) from the local government, the average annual precipitation is 483 mm, and the maximum and minimum annual precipitations are 270 mm (1997) and 774 mm (2020), respectively (Fig. 2a). The cumulative precipitation in 2020 is also the largest ever recorded in this area. This means the maximum annual precipitation is 2.87 times of the minimum and annual precipitation shows significant interannual variation. A maximum daily precipitation of 79.2 mm was recorded on 7 August 2017 (Fig. 2a) although the annual precipitation in 2017 is mediocre.

Meanwhile, the daily precipitation and monthly precipitation extremely varies within a year. The day with daily precipitation higher than 0.1 mm is 96 per year, and the average cumulative precipitation (235.6 mm) in the summer season (June to August) accounts for approximately 49% of the average annual precipitation. In particular, the cumulative monthly precipitation in the summer season of 2020 is 500.1 mm, which accounts for approximately 64.6% of its total annual precipitation.

Topography and geomorphology
Wudu district is situated at the intersection area of the Qinba mountain region, the Qinghai-Tibet Plateau, and the Loess Plateau (Zhang et al. 2022). Due to the strong uplift of neotectonic movement and sharp down-cutting of river rush, the formation of the mountain slope, the study area is characterized by interleaving terrain of precipitous mountains and valley basins with a general terrain of high in the northwest and low in the southeast (Guo et al. 2020) (Fig. 1b). The topographical map in Fig. 1 was generated based on the digital elevation model (DEM) from the ALOS PALSAR DEM and the resolution is 12.5 m. The dominant elevation of the study area is between 1500 and 3000 m. The area with elevation lower than 1500 m is mainly distributed along the Bailong river and its tributaries and the area with elevation higher than 3000 m is mainly distributed at the northwest side of the study area. In terms of the slope gradient, the northeast side of the study area is characterized by gentle topography and its south is characterized by steep topography generally (Fig. 3a). The dominant slope gradient is between 10° and 40°, which accounts for 83.5% of

Fig. 3 Slope gradient (**a**), slope aspect (**b**), and morphotectonics (**c**) of the study area
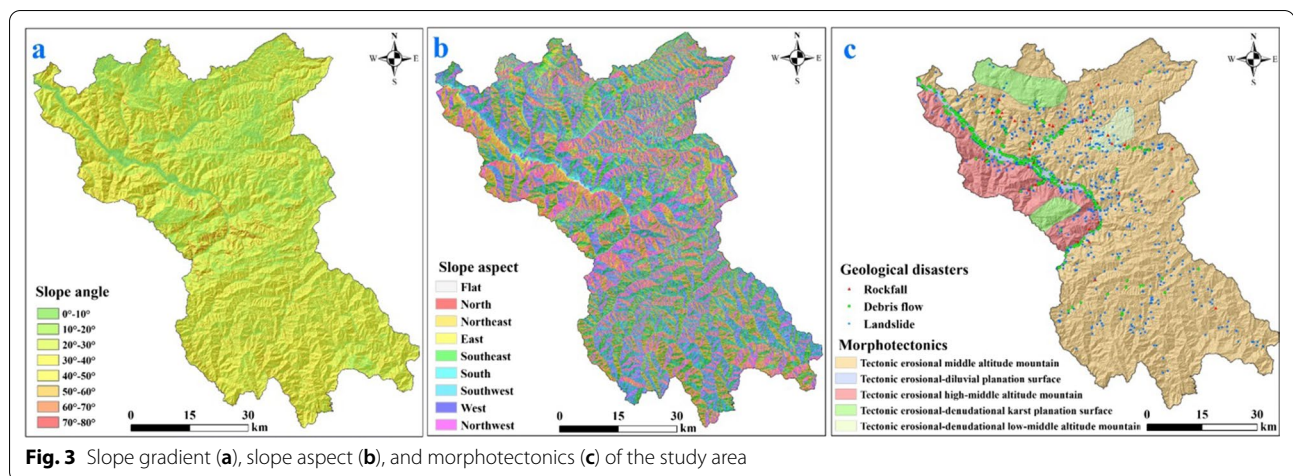
the total study area. The areas with slope gradient lower than 10° and higher than 40° are limited and their area percentages are 11.5% and 4.9%, respectively. The Bailong River valley shows very smooth terrain while its both banks are characterized by steep terrain with slope angle higher than 40°. As to the slope aspect, slopes with four aspects (north, south, east, and west) are nearly even distributed (Fig. 3b). Since the main streams in the study area are developed in nearly east-west direction, west-facing and southwest-facing slopes stand out slightly in the study area.

The morphotectonics of the study area is complicated and can be generally divided into five units,, i.e., tectonic erosional-diluvial planation surface, tectonic erosional-denudational low-middle altitude mountain, tectonic erosional middle altitude mountain, tectonic erosional high-middle altitude mountain, tectonic erosional-denudational karst planation surface (Fig. 3c). The tectonic erosional-diluvial planation surface is mainly distributed along the Bailong River and its tributaries and composed of diluvial riverbed, floodplain, river terraces, and proluvial fan. The river valley area is the most concentrated area of towns and population, and important transportation routes are mainly distributed in this area. The tectonic erosional-denudational low-middle altitude mountain is underlain by Neogene red beds and karst. The elevation ranges from 1650 to 2190 m and the relative relief is approximately 200 to 400 m. The slope is relatively gentle with slope angle lower than 25°. The tectonic erosional middle altitude mountain is the most widespread landform type in the region. The elevation ranges from 900 m to 2800 and the relative relief is approximately 500 to 1000 m. This area is generally characterized by sharp relief and steep topography with slope gradient around 30°. The tectonic erosional high-middle altitude mountain is characterized by high relative relief and

steep topography with deeply incised valleys. The relative relief is larger than 1000 m with elevation between 1000 and 3500 m, and the slope gradient is generally higher than 30°. The tectonic erosional-denudational karst planation surface is located at northwest of the study area with elevation higher than 2500 m. While the relative relief is lower with well-developed karst depression, karst cone, sink hole, and karst cave.

Geological and seismic setting

Wudu District is located in the western section of the Qinling orogenic belt which is a part of the Qinqikun orogenic system (Ouyang et al. 2019). In terms of plate tectonics, the study area belongs to the intersection of the Qiangtang block, the Yangtze block and the Qinqikun orogenic system. Meanwhile, the study area is also situated in the Western Qinling-Songpan-Ganzi tectonic region, which is strategically located at convergence region of the east-west Qinling orogenic belt, the nearly north-south Sichuan-Yunnan-Helan tectonic belt and the northeastern Qinghai-Tibet Plateau (Zheng et al. 2010; Zhang et al. 2015). Affected by the regional structure, a complex tectonic system has been formed in the region, which is connected and transformed by the nearly NWW and NW-trending structures. This tectonic pattern determines the landform and stratigraphic distribution characteristics of Wudu District.

Based on the 1:200,000 geological map of the study area, the outcropped strata in the survey area mainly consist of Upper Proterozoic Qingbaikou, Paleozoic Silurian, Devonian, Carboniferous, Permian, Mesozoic Triassic, Jurassic, Cretaceous and Cenozoic Paleogene, Neogene, Quaternary (Dong et al. 2016; Ouyang et al. 2019; Li et al. 2020; Zhang et al. 2022) (Fig. 4a). The Upper Proterozoic Qingbaikou (Qb) strata are distributed in the south of the study area and are composed
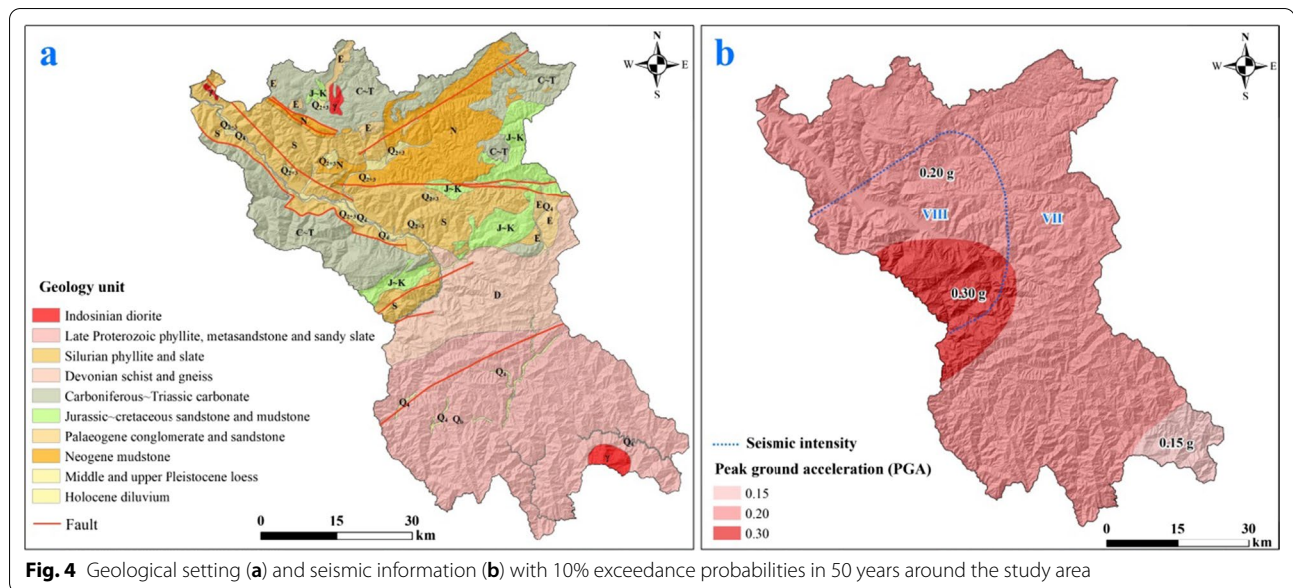
Fig. 4 Geological setting (**a**) and seismic information (**b**) with 10% exceedance probabilities in 50 years around the study area

of Late Proterozoic phyllite, metasandstone and sandy slate. The Lower Paleozoic Silurian strata mainly comprise phyllite, slate and metamorphic sandstone. The Upper Paleozoic Devonian stratum is mainly composed of schist, gneiss, and phyllite. The lithology of Carboniferous, Permian, and Triassic stratum are mainly carbonated rock. The Jurassic and cretaceous strata are mainly sandstone and mudstone. The Cenozoic Paleogene strata are sporadically exposed, and the lithology is purple-red conglomerate, sandstone, and sandy mudstone. The Neogene strata in the area extends in NEE direction and can be divided into upper and lower sections. The lower part of the lower section is purplish red, gray conglomerate and brick red mudstone, and the upper part is gray-green and brown-red mudstone; the lower part of the upper section is interbedded with brown-red mudstone and gray-white glutenite, and the upper part is red mudstone with calcicolous concretion. Generally, the conglomerate increases significantly from west to east. Quaternary strata are mainly distributed around the main stream of Bailong River and the main tributary valleys. The Quaternary system in the region is divided into Middle-Upper Pleistocene, Upper Pleistocene and Holocene according to its formation age and genesis type. The Middle-Upper Pleistocene and Upper Pleistocene consist of aeolian loess, purple-red clay, and alluvial-proluvial gray sand and gravel. The Holocene is mainly composed of alluvial-pluvial sand, gravel, sandy soil, sandy mud, a small amount of breccia-containing silt, silty clay, and widely distributed residual slope deposits. Intrusive rock (Indosinian diorite) with porphyritic texture and massive structure can

be merely observed at the northwest and southeast of the study area.

The study area, situated in the Huining-Wudu north–south seismic belt and is strongly influenced by the Songpan-Pingwu seismic belt, is one of the most seismically active regions in mainland China (Ouyang et al. 2019). Historical earthquakes occurred along active faults, such as the Guanggaishan-Dieshan fault zone, the Diebu-Bailongjiang seismic zone, and the Wenxian-Kangxian fault zone (Du et al. 2017; Zhang et al. 2021). 15 strong earthquakes with magnitude 7 or above were recorded in this area (Ouyang et al. 2019). The seismic intensity of the study area is VII–VIII with 10% exceedance probabilities in 50 years and the corresponding peak ground acceleration is between 0.15 and 0.30 g (Fig. 4b). The active faults and strong earthquakes are two main causes of densely developed geohazards in the study area.

Research methods

The methods applied to support our findings in this work are common and reproducible. For the benefit of easy understanding, we present the explanations pertinent to the methods in a brief way. Correlation analysis between geohazard distribution and topographic factors, geological factors, geomorphological factors as well as triggering factors were carried out using the ArcGIS 10.6 platform, and depicted through Grapher 14.0. The landslides, debris flows, and collapses in each class (unit) were classified with the select by location tool in ArcGIS and the corresponding percentage were calculated respectively. Two indicators, i.e., class area percentage, geohazard (landslide, debris flow, and collapse) number percentage,

Zhang *et al. Geoenvironmental Disasters*   (2022) 9:23

Page 6 of 19

are listed in Eqs. (1) and (2). The indicator, density index of geohazard (landslide, debris flow, and collapse), stands for the number density of geohazard in a given class, and the corresponding equation is listed in Eq. (3).

$$\text{Class area percentage} = \frac{\text{Certain class area}}{\text{Total area}} \times 100\% \tag{1}$$

$$\text{Landslide number percentage} = \frac{\text{Landslide number in a class}}{\text{Total landslide number}} \times 100\% \tag{2}$$

$$\text{Density index of landslide} = \frac{\text{Landslide number percentage}}{\text{Class area percentage}} \tag{3}$$

Equations (2) and (3) are applicable to debris flow and collapse as well. It should be noted that when the density index is larger than 1, it means geohazards developed in this unit is higher than the average of whole study area.

Geohazard type and distribution
Geohazard type
The middle reaches of the Bailong River, where Wudu District is located, is one of the regions with extremely developed geohazards in China. In this work, 1144 geohazards were identified including 759 landslides, 281 debris flows, and 104 collapses (Fig. 5). The geohazard inventory was generated based on the database provided by the local government including 516 geohazards triggered by the 2008 Wenchuan Earthquake and geohazards induced by the 2020 heavy precipitation. Nearly all 1141 geohazards presented in this work were checked onsite in 2020 and 2021. The corresponding number percentages are 66.35%, 24.56%, and 9.09%, respectively.

Landslide is the predominant type of geohazards in the study area (Bai et al. 2011; Bai et al. 2014). Based on the material (composition), thickness of sliding mass, mode of movement, and scale (Scheidegger and Ai 1987; Walke et al. 1987; Hungr et al. 2014), landslides developed in the study area can be classified to different types and the corresponding number and percentage are listed in Table 1.

Rock landslides, generally controlled by discontinuity of rock mass (soft interlayer or joint fissure plane), are often induced by fault activity or seismic activity (Tang et al. 2017; Zhang et al. 2020). This type of landslide is generally characterized by large scale (huge and large), great thickness (deep and intermediate), and rapid movement (Fig. 6a). Earth landslide with a number percentage of 89.46% is a major type of landslide in the study area and usually occurs in Quaternary loose deposits (Fig. 6b).

Collapse in the study area can be classified as earth collapse and rock collapse according to the material and composition (Ma et al. 2022). There are 61 rock collapses in the study area and the number percentage is 58.65%.

Rock collapse commonly occurs in pull-splitting and toppling mode. This type of collapse is generally developed in high-middle altitude mountain that is characterized by steep topography and well-developed joint (Fig. 6c). Earth collapse, generally occurred in area with slope gradient higher than 55°, accounts for 41.35% of all collapses (Table 2). This type of collapse is a major threat to the local residents as earth collapse is predominantly developed in the densely populated area (Fig. 6d).

Debris flow is well-developed in Wudu District and is characterized by dense distribution and abrupt occurrence (Ni et al. 2014). 281 debris flow are identified in this work and account for 24.56% of all geohazards. The density of debris flow is 6.1 per 100 km^2. According to the material composition, watershed shape, fluid properties, development stage and scale, debris flows in the study area can be classified to different types (Rogelis and Werner 2014) (Table 3). Mudflow is the predominant type of debris flow and its total number is 259 accounting for 92.17% of all debris flows in the study area. Mud flows are widely distributed in this region and concentrated along the Bailong River (Fig. 5). Mudflows are mostly developed in gullies with high occurrence frequency and simultaneous occurrence (Fig. 6e, f). Water-rock flow with a total number of 22 (accounting for 7.83%) is sparsely distributed in this region and mainly distributed at the south and northeast mountainous area. Water-rock flows are generally well-forested and occur in low frequency. In terms of the fluid property, viscous debris flows account for 90.39% and is characterized by high solid contents and strong schlep ability. Diluted debris flow with a number percentage of 9.61% is mainly concentrated at the south study area. Diluted debris flow is characterized by low solid contents and weak schlep ability.

Geohazard distribution
The study area with complex geological condition and steep topography has long been afflicted by frequent occurrence of geohazards (Li et al. 2022). The extreme weather and strong earthquakes exacerbate this situation (Zhang et al. 2019; Zhang and Wang 2019; Wang et al. 2021). Geohazards in the study area are characterized by periodicity, frequent occurrence, abrupt occurrence, massive occurrence, and unevenly spatial distribution. Since the occurrence of geohazards in the study area is closely related to torrential precipitation and strong seismic motion, geohazards (especially massive geohazards) are strongly controlled by recurrence period of heavy rainfall and earthquakes (Bai et al. 2011). Meanwhile, affected by the slope structure, material composition and topographical difference, geohazards are unevenly distributed (Qi et al. 2010). In addition, human activities
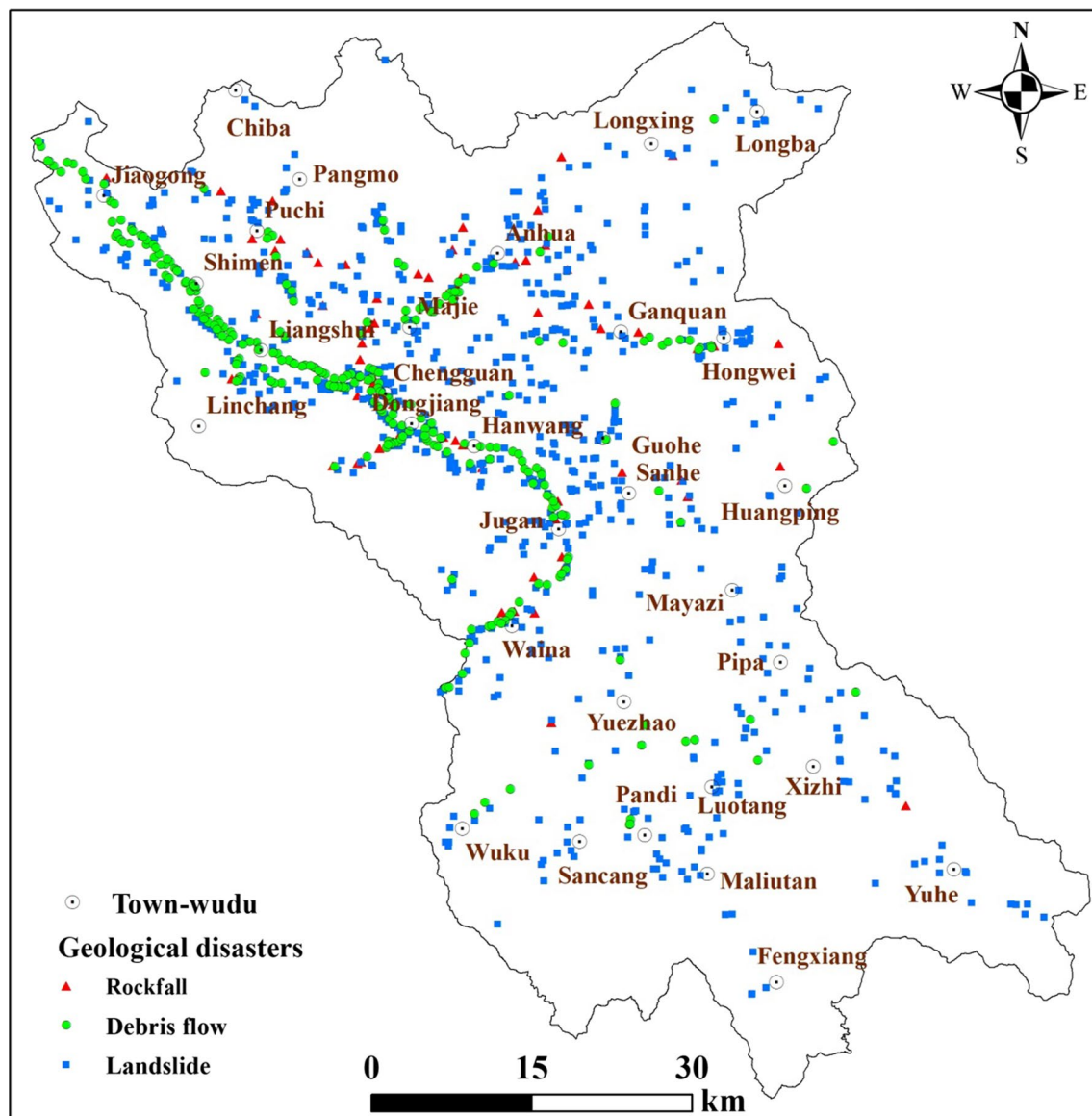
Fig. 5 Geohazards in the study area

and engineering process occasionally give rise to abrupt occurrence of geohazard. In summary, geohazards in Wudu district mainly occur in the summer season and are significantly affected by the topographic feature, geological setting and human engineering activities.

In terms of spatial distribution, debris flows are developed along the Bailong River and its tributaries (Fig. 5). While landslides and collapses are developed in area with high relief (rather than high altitude) where is covered by Quaternary loose deposits and underlain by metamorphic rocks. The high-middle altitude mountainous region with high altitude is characterized by sparse landslides

and collapses. Geohazards are concentrated more on area with strong tectonic movement and along river valleys. Moreover, the distribution of geohazards in the study area is closely related to human engineering activities. Geohazards are densely distributed along roads where is frequently afflicted by engineering disturbance. As the geohazards in the study area are predominantly induced by heavy rainfall and seismic motion, their occurrence and distribution are closely related to the occurrence of extreme rainfall event and seismic event. The temporal distribution of geohazards shows high consistency with the return period of extreme rainfall event and strong

Fig. 6 Typical geohazards in the study area. **a** Rock slide. **b** Earth slide. **c** Rock collapse. **d** Loess collapse. **e** Rainfall-induced debris flow. **f** Dammed river

earthquake. In addition, more than 90% of geohazards occurred between May and September.

Correlation analysis results

The occurrence and distribution of geohazards are jointly controlled by the hazard-inducing environment and triggering factors (Peng et al. 2015; Gao and Sang 2017; Zhang and Wang 2019). The topographic feature, geological setting, and tectonic background are three main hazard-inducing environmental factors and precipitation and earthquake are two major inducing factors (Jia et al. 2019).

Topographical factor

Macroscopically, topography is shaped by the endogenic process and exogenic process, especially the action of neotectonic movement (Zhang et al. 2020; Zhou et al. 2021). The topographic features are mainly reflected in the landform, elevation, relative relief and slope gradient (Zhang et al. 2019). Favorable topographical condition is the primary factor for the formation of geohazards and they are mainly developed in mountainous areas with large topographic relief, strong down-cutting, and densely developed valleys. Topography determines the

Table 1 Type of landslide in the study area

Classification basis	Type	Number	Percentage (%)
Material	Earth slide	679	89.46
	Rock slide	80	10.54
Thickness of sliding mass	Ultra-deep landslide	1	0.13
	Deep landslide	4	0.53
	Intermediate landslide	74	9.75
	Shallow landslide	680	89.59
Mode of movement	Thrust load-caused landslide	556	73.25
	Retrogressive landslide	203	26.75
Scale	Huge landslide	7	0.98
	Large landside	34	4.42
	Medium landslide	260	34.32
	Small landslide	458	60.28

Table 2 Type of collapse in the study area

Classification basis	Type	Number	Percentage (%)
Material	Earth collapse	43	41.35
	Rock collapse	61	58.65
Scale	Large collapse	8	7.69
	Medium collapse	23	22.12
	Small collapse	73	70.19
Mode of movement	Toppling collapse	19	18.27
	Sliding collapse	42	40.38
	Pull-splitting collapse	43	41.35

Table 3 Type of debris flow in the study area

Classification basis	Type	Number	Percentage (%)
Material	Mud flow	259	92.17
	Water-rock flow	22	7.83
Watershed feature	Gully debris flow	247	87.90
	Slope debris flow	34	12.10
Fluid property	Viscous debris flow	254	90.39
	Diluted debris flow	27	9.61
Development stage	Budding debris flow	183	65.12
	Vigorous debris flow	57	20.28
	Degenerating debris flow	20	7.12
	Resting debris flow	21	7.47
Scale	Huge debris flow	14	4.98
	Large debris flow	48	17.08
	Medium debris flow	98	34.88
	Small debris flow	121	43.06

spatial condition for the development, motion and accumulation of geohazards. Moreover, the steep terrain provides the necessary potential energy and material accumulation conditions for the formation of geohazards, and the high gradient ratio along valleys is also the necessary condition for debris flow occurrence.

As the primary geohazard, landslides are obviously controlled by the topographic feature of the study area. Topographic factors such as elevation, slope angle, and slope aspect have been widely used in previous studies to evaluate the influence of such factors on geohazard distribution (Zhang et al. 2019). In this work, the slope height is classified into 9 classes, and number and percentage of landslides in each class is presented (Fig. 7a). Both landslide number and percentage show a descending trend with increasing slope height. The class with slope height below 100 m registers the largest coverage of landslide occurrence though the area with slope height between 201 and 400 m occupies more than half of the study area. This may imply that landslides mainly occur in relatively low and steep slopes where human activity is frequent while few landslides occur in high-altitude region. As to the slope gradient, the study area is predominantly covered by classes with a slope angle between 21° and 40° and the corresponding percentage is 62.4% (Fig. 7b). Not unexpectedly, the dominant slope angle for landslide occurrence is 21°–40° as well and the corresponding landslide number percentage is 72.5% which is slightly higher than the percentage the slope with a gradient between 21° and 40°. This means the slope gradient between 21° and 40° is the advantageous gradient for landslide occurrence. The slope type in the study area can be classified into convex slope, concave slope, step slope,

Zhang *et al. Geoenvironmental Disasters*   (2022) 9:23

Page 10 of 19

Fig. 7 Relationships between landslides and terrain variables. **a** Landslide versus slope height. **b** Landslide versus slope gradient. **c** Landslide versus slope type. **d** Landslide versus mean slope aspect
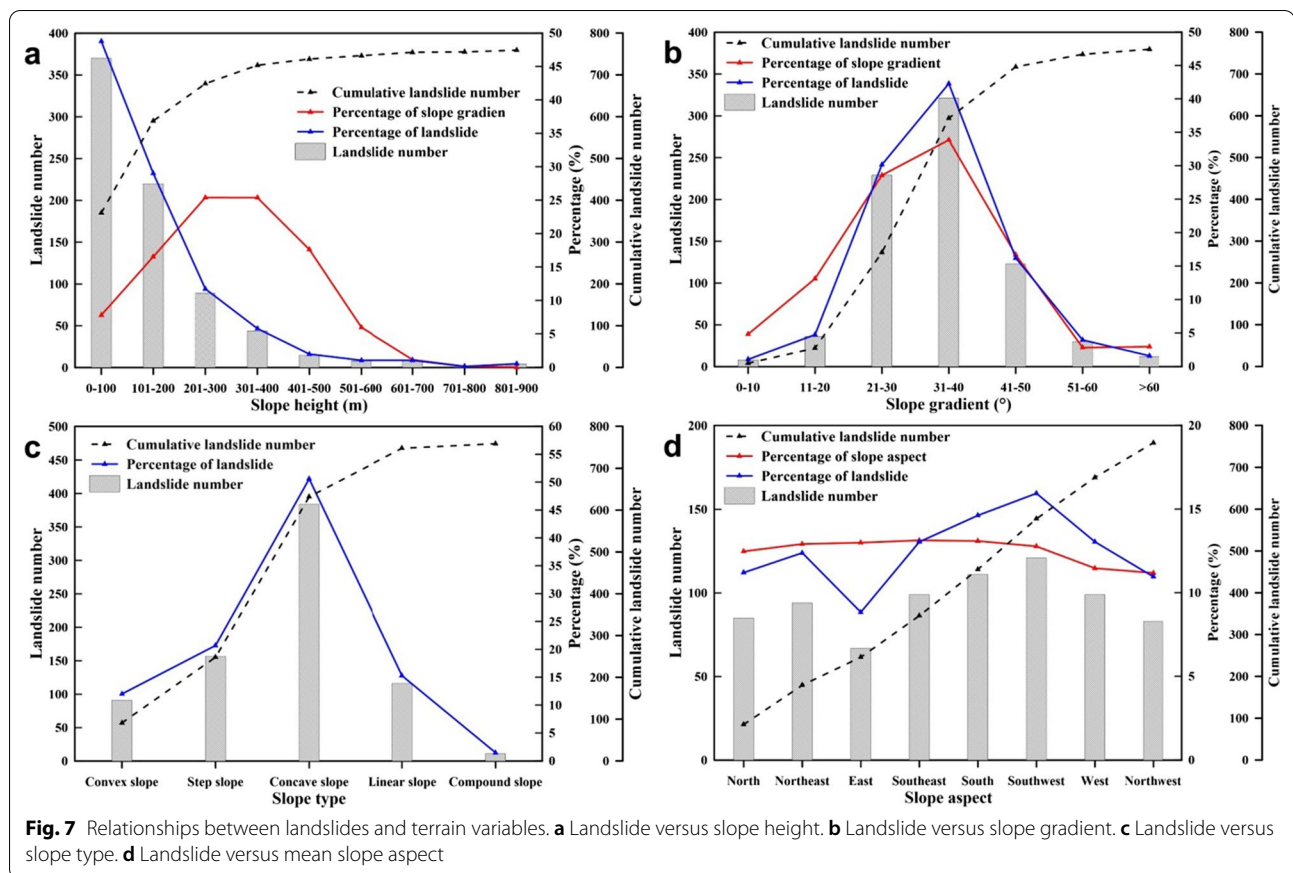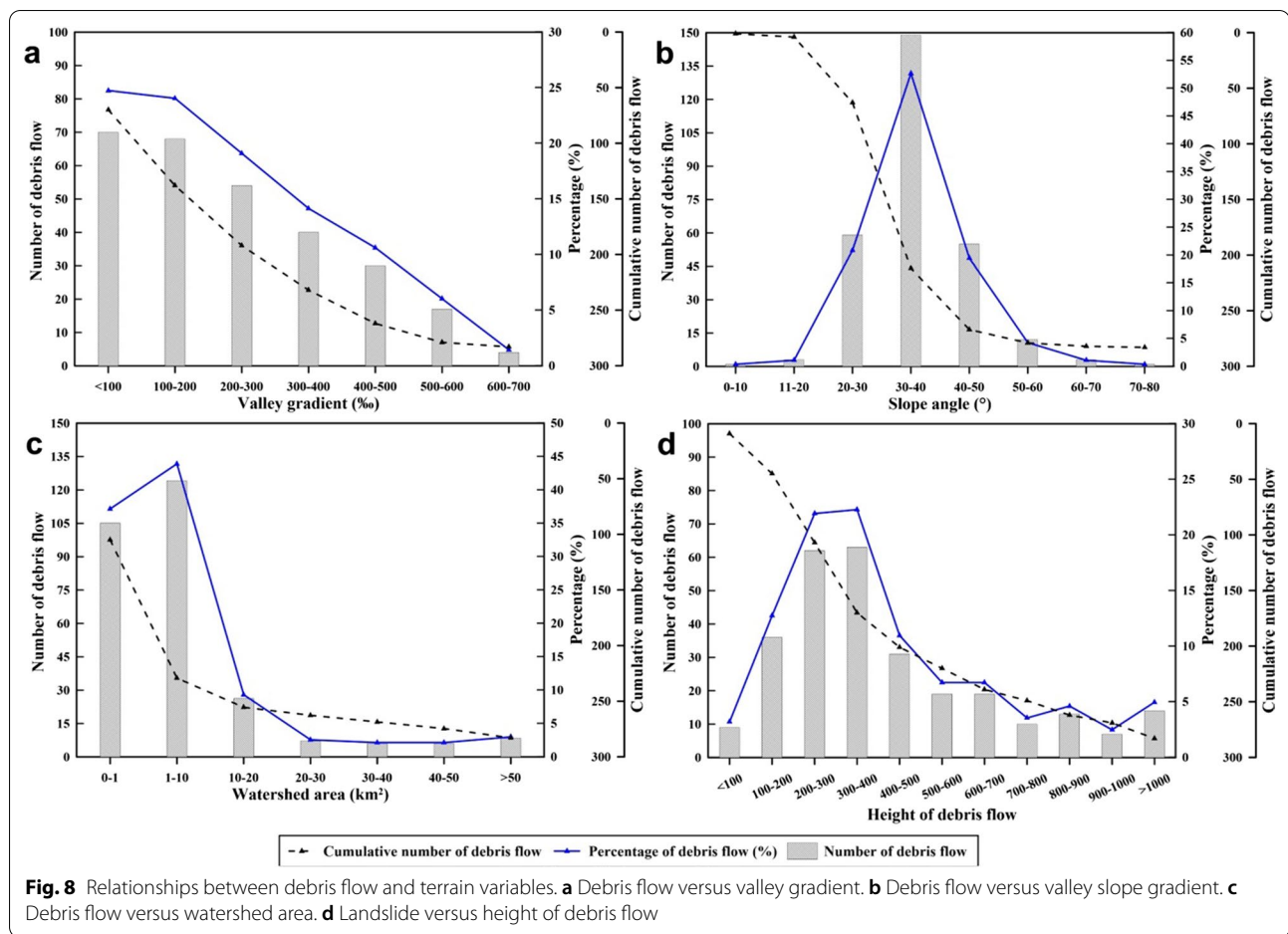
linear slope, and compound slope. The result in Fig. 7c indicates that the preferred slope type is concave slope with a landslide number percentage of 50.6%. Another topographic factor is slope aspect and the slope with different aspect is almost evenly distributed in the study area. Southern-facing and easterly-facing slopes with southeast, south, and east octants stand out slightly in the study area. The corresponding percentages are 13.1%, 13.1%, and 13.0%, marginally larger than the average value of 12.5% (Fig. 7d). While the preferred inclinations of landslides are southwest, south, west, and southeast as illustrated by the distribution curve of number and percentage of landslide (Fig. 7d). Therefore, southwest, south, west, and southeast can be confirmed as the overriding orientation for landslide occurrence in the study area.

Collapse as one type of geohazards with larger vertical displacement than horizontal displacement is obviously controlled by topographic feature. Slope height and slope gradient are two major factors controlling collapse occurrence (Zhang and Liu 2010). Since the collapse is usually characterized by small size compared with landslide and debris flow, it is difficult to quantitatively assess the controlling role of topography on collapse occurrence. Based

on our field investigation, most collapses in the study area occurred in slopes with gradient higher than 45°. As to slope height, the preferred slope heigh shows great difference due to the difference in material composition and structure of slope. Naturally formed steep loess slope with height more than 10 m shows high stability for long time without earthquake and infiltration, while artificial steep loess slope is prone to collapse when the slope heigh is higher than 6 m. This can be attributed to the rapid release of horizontal stress. Neogene mudstone slope widely distributed in the study area is susceptible to collapse as the Neogene mudstone can be easily weathered and joint fissure are well developed.

Topography is the preliminary and necessary condition for the formation of debris flow (Van et al. 2016). Topographic feature controls the formation, motion and accumulation of debris flow and affects the scale and mobility of debris flow (Kean et al. 2013). The controlling effects of topography and landforms on debris flow disasters are mainly manifested in six aspects, i.e., valley gradient, slope angle, watershed area, relative relief, gully density, and watershed shape. Among them, the first four factors are main controlling factors. Valley gradient is a prerequisite for the transformation from

Fig. 8 Relationships between debris flow and terrain variables. **a** Debris flow versus valley gradient. **b** Debris flow versus valley slope gradient. **c** Debris flow versus watershed area. **d** Landslide versus height of debris flow

potential energy to kinetic energy of debris flow source and reflects the developing stage of the debris flow. Based on the statistical analysis, it can be concluded that debris flows are favorably developed and formed in valleys with valley gradient less than 400‰ and the debris flow shows a descending trend with increasing valley gradient (Fig. 8a). This may indicate that the valleys with valley gradient in this range can provide a favorable terrain condition for loose deposit at the source and enough energy for long-runout motion. The slope angle of slopes on both sides of the valley directly affects the scale of debris flow as it controls the quantity of solid source and velocity of overland flow during heavy precipitation. As is illustrated in Fig. 8b, the advantageous slope angle of slopes with the watershed is 30°–40° with a number of debris flow of 149 accounting for 52.7% (Fig. 8b). The following slope angle range is 20°–30° and 40°–50°, and the corresponding percentages are 20.9% and 19.4%, respectively. Combined with field investigation, it is inferred that the most favorable slope gradient for the supply of solid source and overland flow at the debris flow source area is 25°–45°. Generally, the watershed area reflects the

developing stage of debris flow and the larger watershed area usually means broader valley. Thus, debris flow may have a higher possibility to occur in valleys with relatively small watershed area. According to the analysis results, the number of debris flows occurred in valleys with a watershed area of 1–10 km^2 is 124 accounts for 43.9%, following by a watershed area of < 1 km^2 with a number percentage of 37.1% (Fig. 8c). The number of debris flow with area larger than 10 km^2 is only 54. Height of debris flow indicates the relief fluctuation and erosional degree, and reflects the developing stage of valley to some extent. Most debris flow occurred in valleys with heigh between 100 and 500 m and the total number of the debris flow developed within this range is 192 accounting for 67.9% of all (Fig. 9d). While debris flow developed with height larger than 500 m only registers 29.0%.

Geological factor
Lithology is one of the most important controlling factors for the development of geohazards. The controlling role of lithology on geological disasters is mainly reflected in the mechanical properties of rock and soil
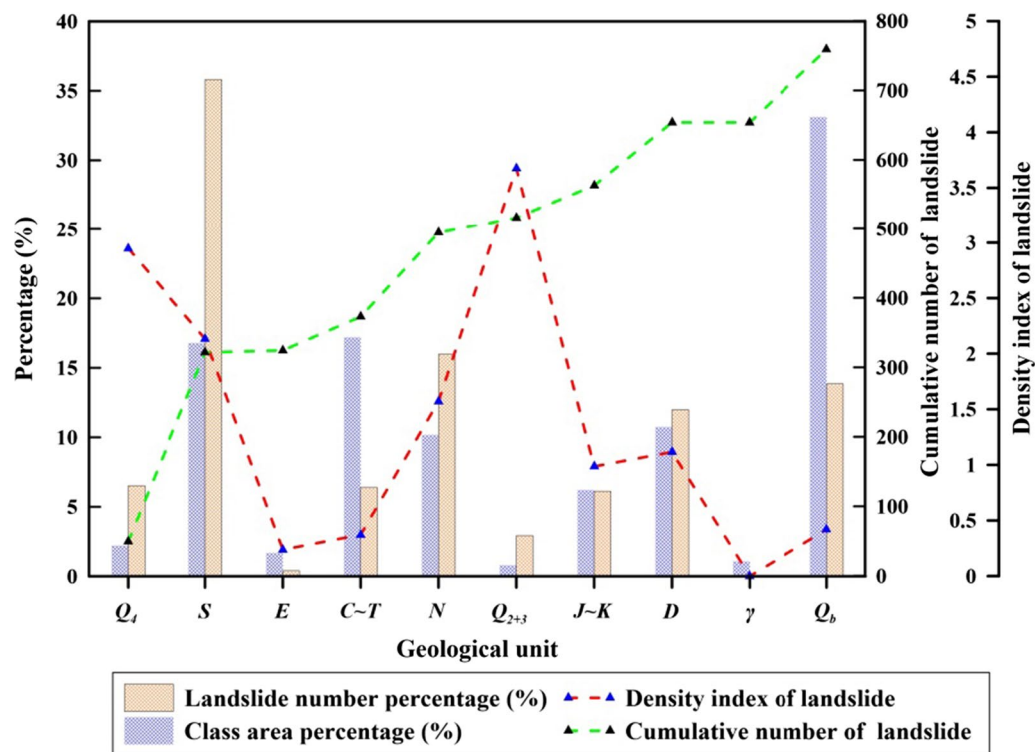
Zhang *et al. Geoenvironmental Disasters*   (2022) 9:23

Page 12 of 19

Fig. 9 Relationships between landslide and geological unit

which are material basis of slopes (Wen et al. 2004). To effectively evaluate the preference of geohazards developed in different geological unit, the density index was used to evaluate the number density of geohazards in each unit. In this work, the geology units in the study area were divided into 10 classes (Fig. 4a) and geohazards developed in each unit were further analyzed (Fig. 9). Q_b (Late Proterozoic phyllite, metasandstone and sandy slate) is the largest class with a CAP of 43.0%. The following classes are C–T (Carboniferous–Triassic carbonate), S (Silurian phyllite and slate), D (Devonian schist and gneiss), and N (Neogene mudstone) and their class area percentages are 17.2%, 16.8%, 10.7%, 10.2% (Fig. 9).

In terms of landslides, class S is the geological unit with most landslide occurrence with a landslide number percentage of 35.8% (Fig. 9). The following geological units with massive landslide occurrence are classes N, Q_b, and D, and the corresponding landslide number percentages are 16.0%, 13.9%, and 12.0, respectively. While the class with most abundant landslide occurrence appears in class Q_{2+3} (Middle and upper Pleistocene loess) with density index of 3.68. This means the number density of landslides developed in Middle and upper Pleistocene loess is 3.68 times of that of the whole study area (Fig. 9). The classes with density index higher than 1 incorporate Q_4, S, N, and D and their density indexes are 2.95, 2.13,

1.57 and 1.12. The statistical analysis indicates that slopes with Middle and upper Pleistocene loess, Holocene diluvium, Silurian phyllite and slate, Neogene mudstone, and Devonian schist and gneiss are prone to landslide occurrence, which is in accordance with our field observation.

In a similar vein, relationship between collapse (debris flow) occurrence and geological unit was analyzed (Fig. 10). As to collapse, the first four classes registering large collapse number are S, N, Q_4 and D with the number percentage of 38.7%, 30.1%, 8.6% and 6.5%, respectively (Fig. 10). However, classes with number density larger than average appears in Q_{2+3}, Q_4, N and S, and their density indexes are 6.74, 3.89, 2.96, and 2.31. Thus, it is concluded that collapses may predominantly occurred in Quaternary loess, diluvium, and deluvium, Neogene mudstone and sandstone, and Silurian phyllite and slate. This feature is similar to that of landslide occurrence. Debris flow is a major geohazard in the study area and can be roughly classified as mud flow and water-rock flow. The statistical analysis in Fig. 11 indicates the debris flow is prone to occur in area with Quaternary loess, diluvium, and deluvium, Silurian phyllite and slate. In combination to our field investigation, it is preliminarily concluded that mud flows generally occurred at the northwest of the study area long the Bailong River and its tributaries and water-rock flow is more likely to occur in
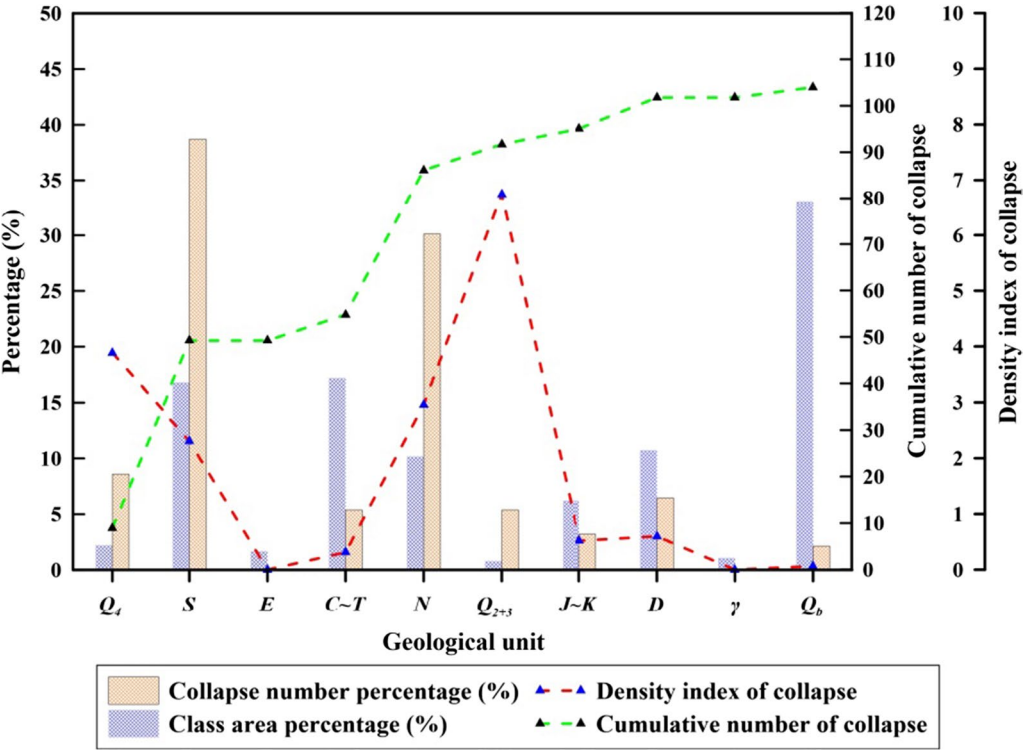
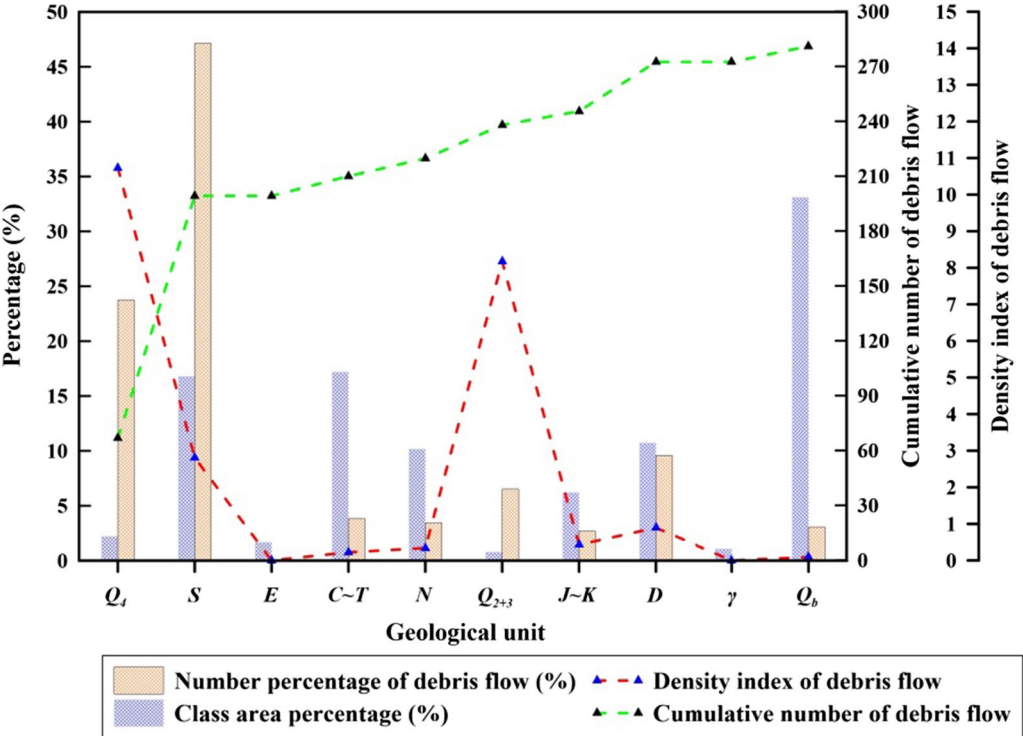**Fig. 10** Relationships between collapse and geological unit

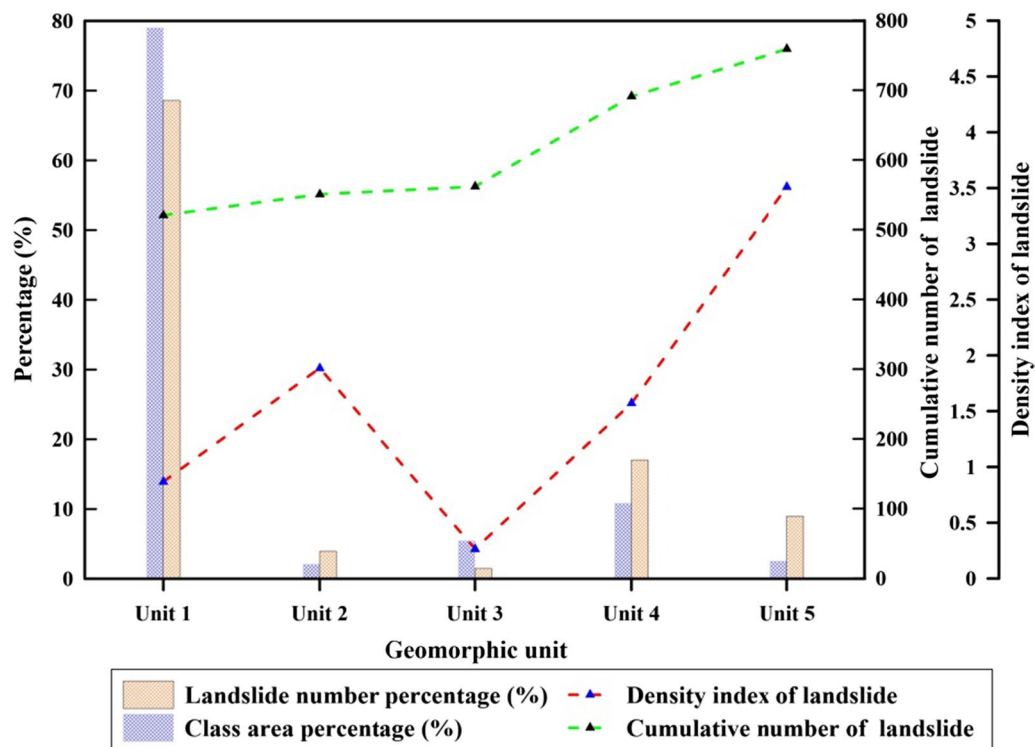**Fig. 11** Relationships between debris flow and geological unit

Fig. 12 Relationships between landslide and geomorphic unit. Unit 1, unit 2, unit 3, unit 4, and unit 5 are tectonic erosional middle altitude mountain, tectonic erosional-denudational low-middle altitude mountain, tectonic erosional-denudational karst planation surface, tectonic erosional high-middle altitude mountain, tectonic erosional-diluvial planation surface, respectively

Silurian phyllite and slate and Late Proterozoic phyllite, metasandstone and sandy slate.

Geomorphological factor

Tectonic geomorphology reflects synthetical effect of the uplift from endogenic process and deplanation from exogenic process (Summerfield 1989). To investigate the controlling role of geomorphological factor on geohazards, correlation analysis was conducted. Tectonic geomorphology can be divided to 5 units, i.e., tectonic erosional middle altitude mountain (unit 1), tectonic erosional-denudational low-middle altitude mountain (unit 2), tectonic erosional–denudational karst planation surface (unit 3), tectonic erosional high-middle altitude mountain (unit 4), tectonic erosional-diluvial planation surface (unit 5) (Figs. 3c, 12, 13 and 14) and the corresponding class area percentages are 79.0%, 2.1%, 5.5%, 10.8%, and 2.6%, respectively. In terms of landslide occurrence and distribution, unit 1, unit 4 and unit 5 register the largest three classes with the landslide number percentages of 68.6%, 17.0% and 9.0%, respectively. While the three units with largest density index are unit 5, unit 2, and unit 4, and their density indexes are 3.51, 1.89, and 1.57 (Fig. 12). This means landslides is prone to occur

in unit 1, unit 5, and unit 4 as most landslides occurred in these units and the density index is relatively high. Occurrence and distribution of collapse and debris flow show similar trend, and nearly all collapses and debris flows occurred in these three units. The collapse number percentages of unit 1, unit 5, and unit 4 are 59.6%, 22.3% and 14.9%, and their density indexes are 0.75, 8.74, and 1.37, respectively (Fig. 13). The debris flow number percentages of unit 5, unit 1 and unit 4 are 52.7%, 27.3% and 19.3%, and their density indexes are 20.62, 1.78 and 0.35, respectively (Fig. 14).

Triggering factors

Triggering factors are the necessary variables controlling the occurrence of geohazards and precipitation is one the most important factors affecting the occurrence of geohazards in the study area (Zhuang et al. 2016). Considering geohazards presented in this work occurred in variable time in history, it is unreasonable to analyze their distribution with a certain precipitation event. In this light, mean annual precipitation was considered. The mean annual precipitation of the study area is classified into 10 classes (Fig. 1c) and correlation between geohazards and mean annual precipitation was conducted
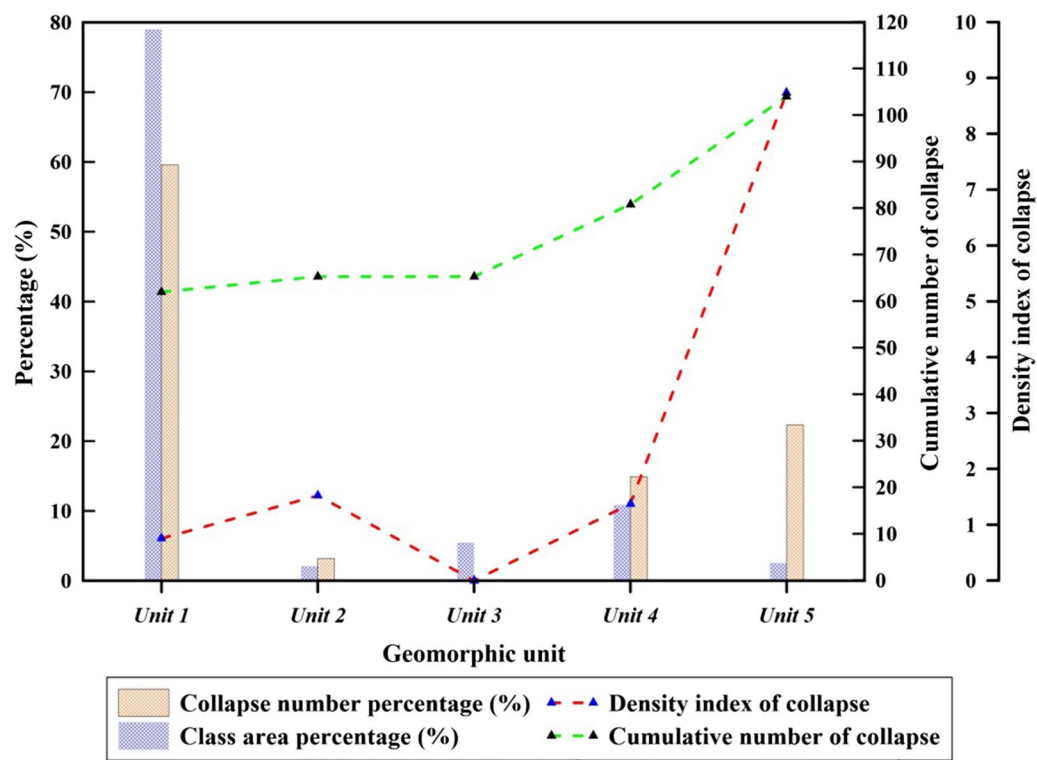
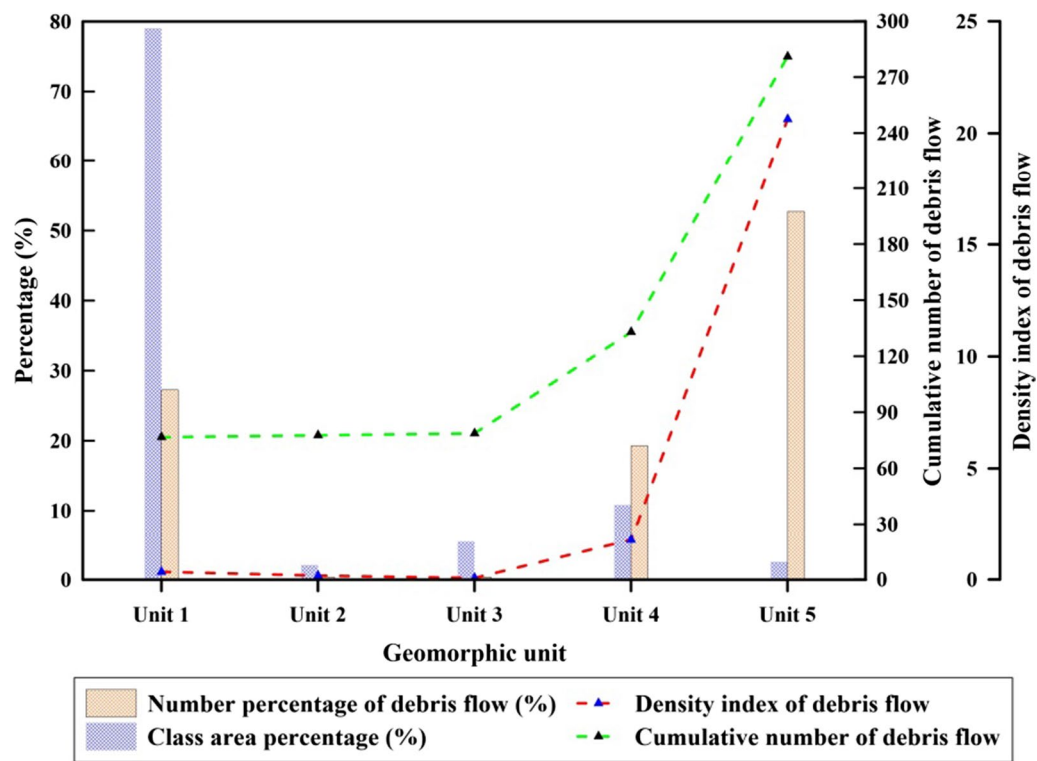**Fig. 13** Relationships between collapse and geomorphic unit

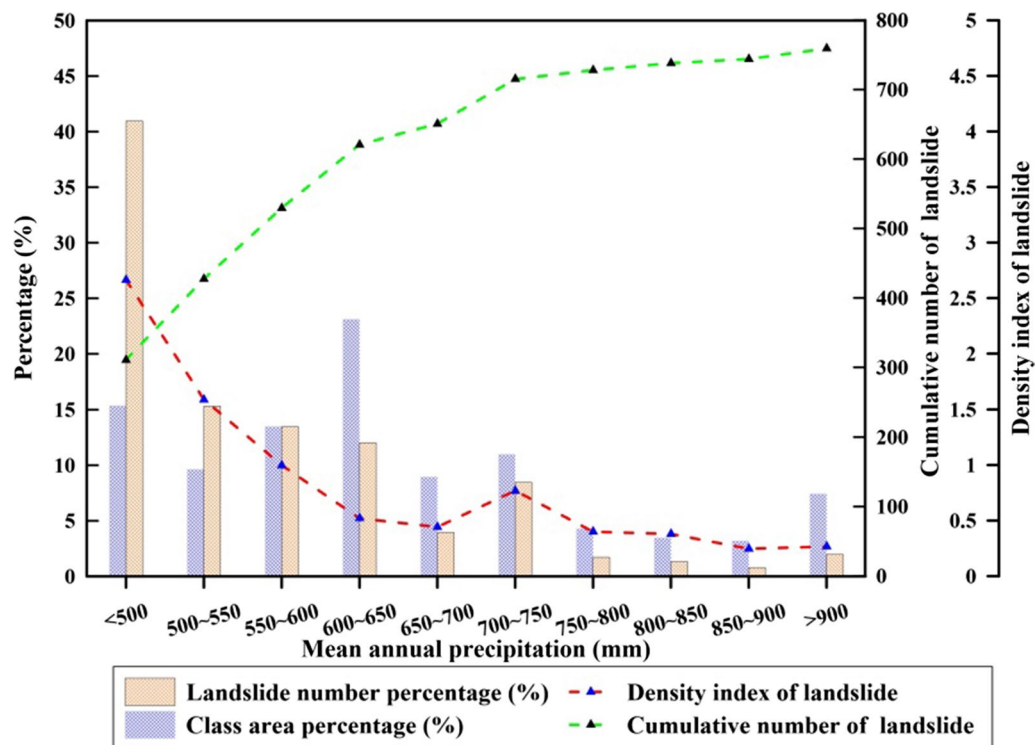**Fig. 14** Relationships between debris flow and geomorphic unit

Fig. 15 Relationships between landslide and mean annual precipitation

(Figs. 15, 16 and 17). The area registering the largest three class area percentage are characterized by mean annual precipitation of 600–650 mm, < 500 mm, and 550–600 m. However, all geohazards including landslides (Fig. 15), collapses (Fig. 16), and debris flows (Fig. 17) show a decreasing trend with the increase of mean annual precipitation, as is illustrated by number percentage and density index of geohazards. This means geohazards are more densely distributed in area with annual precipitation lower than 600 mm. Two reasons may explain this phenomenon. The first one is that geohazards, especially massive geohazards generally occurred in a certain extreme rainfall event and the spatial distribution of the extreme rainfall event may not be completely in accordance with the mean annual precipitation. Another reason is that the area precipitation lower than 600 mm mainly distributed along the Bailong River (Fig. 1c) where is characterized by steep topography and intense human activities. Thus, it may be concluded that mean annual precipitation is not such an important factor controlling geohazards occurrence, and geohazards are controlled directly by rainfall intensity and total amount during extreme rainfall events.

Generally, earthquake controls the occurrence of geohazards in two ways, i.e., coseismic effect and post-earthquake effect (Chen et al. 2020). Strong earthquakes

trigger large amounts of landslides and collapses directly due to the strong seismic motion imposed to the slope. On the other hand, loose soil and rock resulted from strong earthquakes are prone to failure when suffered from heavy rainfall or engineering disturbance. The 2008 Wenchuan earthquake is the most significant earthquake occurred in recent decades around the study area. The seismic intensity of the study area is around VII–VIII and hundreds of geohazards were triggered by this earthquake. The Wenchuan earthquake had a significant impact on the stability of the slopes. The strong vibration during the earthquake loosened the loess blanked in the study area and enhanced the expansion and generation of fissures in rocks which provides channels for precipitation infiltration and runoff. As to debris flow, earthquake generally can not trigger massive debris flow. However, landslides and collapses triggered by strong earthquakes can serve as the solid source for debris flow. Thus, post-earthquake debris flows commonly occur after a succession of heavy rainfall.

In addition to heavy rainfall and strong seismic motion, engineering activities of mankind is another factor frequently resulting in geohazards. Slope-cutting process is a common engineering activity in road construction and house-building during urban expansion. Geohazards triggered by human activity frequently occurred in the
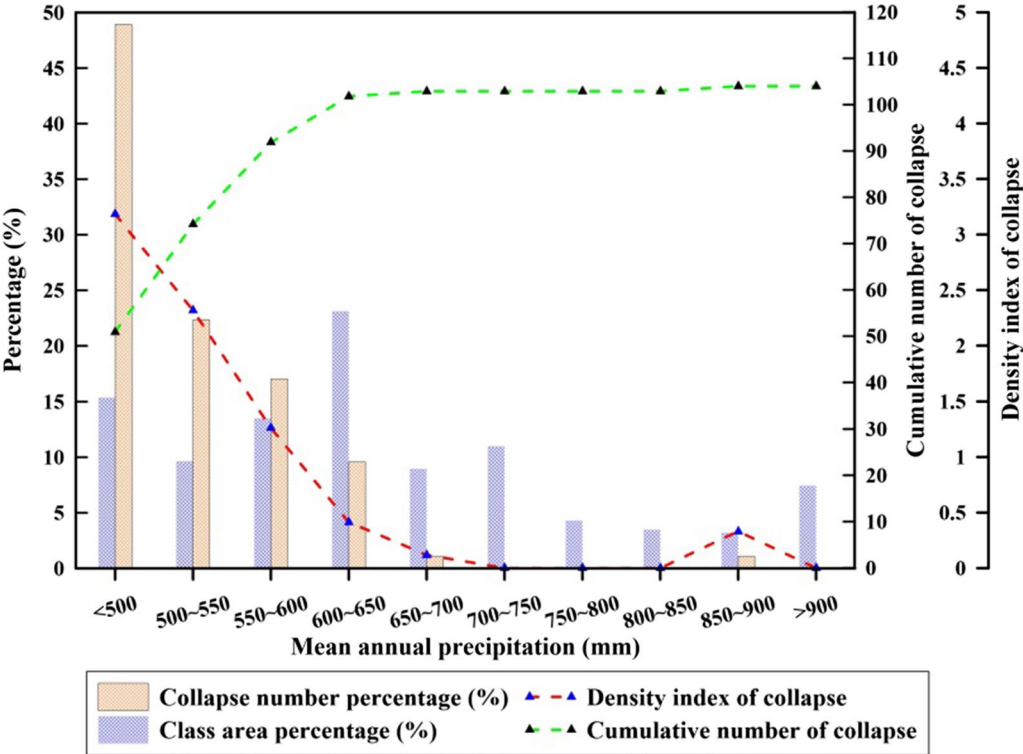
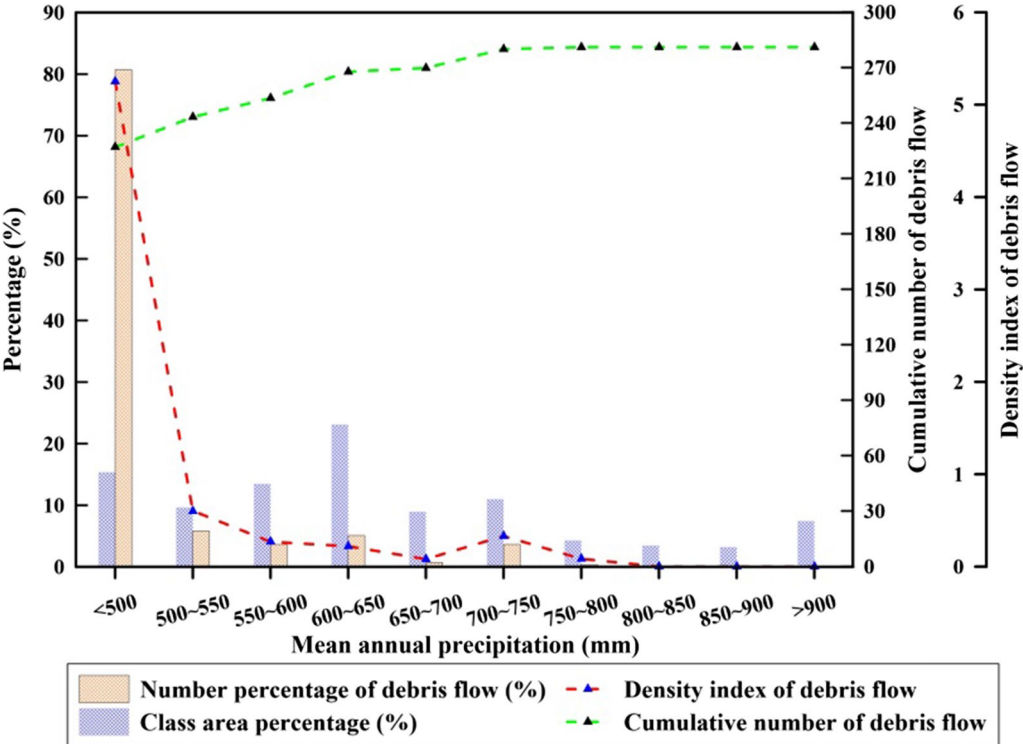**Fig. 16** Relationships between collapse and mean annual precipitation

Fig. 17 Relationships between debris flow and mean annual precipitation

Zhang *et al. Geoenvironmental Disasters* (2022) 9:23

Page 18 of 19

study area, especially along certain segments of national road G345 and G247 and county road X408.

Discussion and conclusion

The middle reaches of the Bailong River, where Wudu district is situated, is the area with the most concentrated geohazard occurrence in Gansu province, China. 1144 geohazards including 759 landslides, 281 debris flows, and 104 collapses in the study area were presented in this work. Geohazards developed in the study area nearly incorporate all types of landslides, collapses, and debris flows, and they are densely distributed along the Bailong River. Correlation analysis result between geohazard distribution and hazard-inducing environment as well as triggering factors indicates the favorable context for geohazard occurrence. For landslides, concave slopes with southwest, south, west, and southeast octants, slope height smaller than 200 m and slope gradient between 21° and 40° is the favorable topographic feature and landslides are prone to occur in Middle and upper Pleistocene loess, Holocene diluvium, Silurian phyllite and slate, Neogene mudstone, and Devonian schist and gneiss. The preferable strata for collapse are similar to that of landslide, and collapses generally occur in slope with gradient larger than 45°. In terms of debris flow, valleys with valley gradient less than 400‰, valley height between 100 and 500 m, and watershed area of 1–10 km^2 register the largest percentage and the most favorable slope gradient for the supply of solid source overland flow at the debris flow source area is 25°~45°. In addition, most landslides, collapses, and debris flows occurred in tectonic erosional middle altitude mountain, tectonic erosional high-middle altitude mountain, tectonic erosional-diluvial planation surface. In terms of triggering factors, mean annual precipitation is not positively corelated with geohazard distribution. This may be contributed to that a certain rainfall event with high intensity may play a more important role than mean annual precipitation. Other reason is inferred to be that human engineering activity makes a favorable condition as geohazards are densely concentrated to well-populated area. In addition, the impact of earthquake on geohazard may decrease the correlation between geohazards distribution and precipitation since geohazards triggered by strong earthquakes were included in the analysis. Although, no quantificationally analysis between earthquake and geohazard was conducted, their controlling role on geohazard occurrence is self-evident. Since most main roads in study area were constructed along the Bailong River and its tributaries, it is difficult to concluded whether the geohazards were triggered by human engineering activity or river erosion. Thus, the influence of human engineering activity and river erosion was not quantitively evaluated in this work.

More investigation on quantitative analysis between triggering factors and geohazard distribution (especially along the Bailong River) will be conducted in our further study.

Based on our field investigation and statistical analysis, it can be concluded that geohazards in the study area are characterized by periodicity, frequent occurrence, abrupt occurrence, massive occurrence, and unevenly spatial distribution and they mainly occurred in rainy season. Macroscopically, development and distribution of geohazards are controlled by regional tectonic stress field and deep faults. Geological setting is the basis for geohazard development and occurrence, and sliding-prone stratum is the internal factor. Steep topography provides favorable condition for geohazard occurrence, and extreme rainfall, strong seismic motion, and human engineering activity enhance the situation.

Author contributions
SZ and PS drafted the manuscript; RL and JR carried out the correlation analysis; YZ conducted the field investigations. All authors read and approved the final manuscript.

Availability of data and materials
The data presented in this study are all available on request.

Declarations

Competing interests
The authors declare that they have no competing interests.

Author details
[1]Institute of Geomechanics, Chinese Academy of Geological Sciences, Beijing 100081, China. [2]Observation and Research Station of Geological Disaster in Baoji, Ministry of Natural Resources, Baoji 721001, Shaanxi, China. [3]Key Laboratory of Active Tectonics and Geological Safety, Ministry of Natural Resources, Beijing 100081, China. [4]Geological Survey of Gansu Province, Lanzhou 730000, China.

References
Bai S, Wang J, Glade T, Bell R, Thiebes B (2011) Rainfall threshold analysis and landslide susceptibility mapping in Wudu county. In: Proceedings of the second world landslide forum, 3–7 October 2011, Rome
Bai S, Wang J, Zhang Z, Cheng C (2012) Combined landslide susceptibility mapping after Wenchuan earthquake at the Zhouqu segment in the Bailongjiang Basin, China. Catena 99:18–25
Bai S, Cheng C, Wang J, Thiebes B, Zhang Z (2013) Regional scale rainfall-and earthquake-triggered landslide susceptibility assessment in Wudu County, China. J Mt Sci 10(5):743–753

Zhang *et al. Geoenvironmental Disasters*   (2022) 9:23

Page 19 of 19

Bai S, Wang J, Thiebes B, Cheng C, Yang Y (2014) Analysis of the relationship of landslide occurrence with rainfall: a case study of Wudu County, China. Arab J Geosci 7(4):1277–1285

Chen M, Tang C, Xiong J, Shi QY, Li N, Gong LF, Wang XD, Tie Y (2020) The long-term evolution of landslide activity near the epicentral area of the 2008 Wenchuan earthquake in China. Geomorphology 367:107317

Dong Y, Yang Z, Liu X, Sun S, Li W, Cheng B, Zhang F, Zhang X, He D, Zhang G (2016) Mesozoic intracontinental orogeny in the Qinling Mountains, central China. Gondwana Res 30:144–158

Du G, Zhang Y, Iqbal J, Yang Z, Yao X (2017) Landslide susceptibility mapping using an integrated model of information value method and logistic regression in the Bailongjiang watershed, Gansu Province, China. J Mt Sci 14(2):249–268

Fan X, Scaringi G, Xu Q, Zhan W, Dai L, Li Y, Pei X, Yang Q, Huang R (2018) Coseismic landslides triggered by the 8th August 2017 Ms 7.0 Jiuzhaigou earthquake (Sichuan, China): factors controlling their spatial distribution and implications for the seismogenic blind fault identification. Landslides 15(5):967–983

Gao J, Sang Y (2017) Identification and estimation of landslide-debris flow disaster risk in primary and middle school campuses in a mountainous area of Southwest China. Int J Disaster Risk Reduct 25:60–71

Gorum T, Fan X, van Westen CJ, Huang RQ, Xu Q, Tang C, Wang G (2011) Distribution pattern of earthquake-induced landslides triggered by the 12 May 2008 Wenchuan earthquake. Geomorphology 133(3–4):152–167

Guo C, Zhang Y, Li X, Ren S, Yang Z, Wu R, Jin J (2020) Reactivation of giant Jiangdingya ancient landslide in Zhouqu county, Gansu province, China. Landslides 17(1):179–190

Hungr O, Leroueil S, Picarelli L (2014) The Varnes classification of landslide types, an update. Landslides 11(2):167–194

Jia H, Chen F, Pan D (2019) Disaster chain analysis of avalanche and landslide and the river blocking dam of the Yarlung Zangbo River in Milin County of Tibet on 17 and 29 October 2018. Int J Environ Res Public Health 16(23):4707

Kean JW, McCoy SW, Tucker GE, Staley DM, Coe JA (2013) Runoff-generated debris flows: observations and modeling of surge initiation, magnitude, and frequency. J Geophys Res Earth Surf 118(4):2190–2207

Li H, Zhang Y, Dong S, Zhang J, Sun Y, Wang Q (2020) Neotectonics of the Bailongjiang and Hanan faults: new insights into late Cenozoic deformation along the eastern margin of the Tibetan Plateau. GSA Bull 132(9–10):1845–1862

Li S, Ni Z, Zhao Y, Hu W, Long Z, Ma H, Zhou G, Luo Y, Geng C (2022) Susceptibility analysis of geohazards in the Longmen Mountain Region after the Wenchuan Earthquake. Int J Environ Res Public Health 19(6):3229

Liu J, Wu Z (2020) Landslide risk assessment of the Zhouqu-Wudu section of Bailong River Basin based on geographic information system. China Earthq Eng J 42(6):1723–1734

Liu Y, Qiu H, Yang D, Liu Z, Ma S, Pei Y, Zhang J, Tang B (2022) Deformation responses of landslides to seasonal rainfall based on InSAR and wavelet analysis. Landslides 19(1):199–210

Ma E, Lai J, Xu S, Shi X, Zhang J, Zhong Y (2022) Failure analysis and treatments of a loess tunnel being constructed in ground fissure area. Eng Fail Anal 134:106034

Ni H, Tang C, Zheng W, Xu R, Tian K, Xu W (2014) An overview of formation mechanism and disaster characteristics of post-seismic debris flows triggered by subsequent rainstorms in Wenchuan earthquake extremely stricken areas. Acta Geologica Sinica (English Edition) 88(4):1310–1328

Ouyang C, Wang Z, An H, Liu X, Wang D (2019) An example of a hazard and risk assessment for debris flows—a case study of Niwan Gully, Wudu, China. Eng Geol 263:105351

Peng J, Fan Z, Wu D, Zhuang J, Dai F, Chen W, Zhao C (2015) Heavy rainfall triggered loess–mudstone landslide and subsequent debris flow in Tianshui, China. Eng Geol 186:79–90

Qi S, Xu Q, Lan H, Zhang B, Liu J (2010) Spatial distribution analysis of landslides triggered by 2008.5. 12 Wenchuan Earthquake. China Eng Geol 116(1–2):95–108

Rogelis MC, Werner M (2014) Regional debris flow susceptibility analysis in mountainous peri-urban areas through morphometric and land cover indicators. Nat Hazards Earth Syst Sci 14(11):3043–3064

Scheidegger AE, Ai NS (1987) Clay slides and debris flow in Wudu region. J Soil Water Conserv 1(2):19–27

Summerfield MA (1989) Tectonic geomorphology: convergent plate boundaries, passive continental margins and supercontinent cycles. Prog Phys Geogr 13:431–4413

Tang H, Yong R, Ez Eldin MA (2017) Stability analysis of stratified rock slopes with spatially variable strength parameters: the case of Qianjiangping landslide. Bull Eng Geol Environ 76(3):839–853

Van Tu T, Duc DM, Tung NM, Cong VD (2016) Preliminary assessments of debris flow hazard in relation to geological environment changes in mountainous regions, North Vietnam. Vietnam J Earth Sci 38(3):277–286

Walker BF, Blong RJ, MacGregor JP (1987) Landslide classification, geomorphology, and site investigations. In: Walker B, Fell R (eds) Soil slope instability and stabilization. Balkema, Rotterdam

Wang F, Zhang S, Li R, Zhou R, Auer A, Ohira H, Dai Z, Inui T (2021) Hydrated halloysite: the pesky stuff responsible for a cascade of landslides triggered by the 2018 Iburi earthquake, Japan. Landslides 18(8):2869–2880

Wen B, Wang S, Wang E, Zhang J (2004) Characteristics of rapid giant landslides in China. Landslides 1(4):247–261

Xie Z, Chen G, Meng X, Zhang Y, Qiao L, Tan L (2017) A comparative study of landslide susceptibility mapping using weight of evidence, logistic regression and support vector machine and evaluated by SBAS-InSAR monitoring: Zhouqu to Wudu segment in Bailong River Basin, China. Environ Earth Sci 76(8):1–9

Xu C, Xu X, Shyu JB (2015) Database and spatial distribution of landslides triggered by the Lushan, China Mw 6.6 earthquake of 20 April 2013. Geomorphology 248:77–92

Zhang M, Liu J (2010) Controlling factors of loess landslides in western China. Environ Earth Sci 59(8):1671–1680

Zhang S, Wang F (2019) Three-dimensional seismic slope stability assessment with the application of Scoops3D and GIS: a case study in Atsuma, Hokkaido. Geoenviron Disasters 6(1):1–14

Zhang Y, Zeng L, Li Z, Wang C, Zhang K, Yang W, Guo T (2015) Late Permian–Triassic siliciclastic provenance, palaeogeography, and crustal growth of the Songpan terrane, eastern Tibetan Plateau: evidence from U–Pb ages, trace elements, and Hf isotopes of detrital zircons. Int Geol Rev 57(2):159–181

Zhang Y, Meng X, Chen G, Qiao L, Zeng R, Chang J (2016) Detection of geohazards in the Bailong River Basin using synthetic aperture radar interferometry. Landslides 13(5):1273–1284

Zhang S, Li R, Wang F, Iio A (2019) Characteristics of landslides triggered by the 2018 Hokkaido Eastern Iburi earthquake, Northern Japan. Landslides 16(9):1691–1708

Zhang S, Yin Y, Hu X, Wang W, Zhu S, Zhang N, Cao S (2020) Initiation mechanism of the Baige landslide on the upper reaches of the Jinsha River, China. Landslides 17(12):2865–2877

Zhang Z, Wang T, Wu S (2020) Distribution and features of landslides in the Tianshui Basin, Northwest China. J Mt Sci 17(3):686–708

Zhang Y, Zheng W, Yuan D, Wang W, Zhang P (2021) Geometrical imagery and kinematic dissipation of the late Cenozoic active faults in the West Qinling Belt: implications for the growth of the Tibetan Plateau. J Geomech 27(2):159–177

Zhang S, Sun P, Zhang Y, Ren J, Wang H (2022) Hazard zonation and risk assessment of a Debris flow under different rainfall condition in Wudu District, Gansu Province, Northwest China. Water 14(17):2680

Zheng W, Griffin WL, Sun M, O'Reilly SY, Zhang H, Zhou H, Xiao L, Tang H, Zhang Z (2010) Tectonic affinity of the west Qinling terrane (central China): North China or Yangtze?. Tectonics 29(2), TC2009

Zhou H, Liu B, Ye F, Fu W, Tang W, Qin Y, Fang T (2021) Landslide distribution and sliding mode control along the Anninghe fault zone at the eastern edge of the Tibetan Plateau. J Mt Sci 18(8):2094–2107

Zhuang J, Peng J, Zhu X, Li W, Ma P, Liu T (2016) Spatial distribution and susceptibility zoning of geohazards along the Silk Road, Xian-Lanzhou. Environ Earth Sci 75(8):1–11

Publisher's Note